PROCEEDINGS OF SCIENCE

# Vertex and Track Reconstruction and Luminosity Monitoring at LHCb

**Jianchun Wang**[1]
*Syracuse University*
*Department of Physics, Syracuse University, Syracuse NY 13244, USA*
*E-mail: jwang@phy.syr.edu*

The VELO detector plays a key role in the LHCb experiment. It is essential in vertex and track reconstruction. It can also be used to monitor luminosity. A brief description on the track reconstruction algorithm and application are given. A subset of the final VELO detector has been tested in a pion beam at CERN. Some preliminary results are presented.

*The 16th International Workshop on Vertex detectors*
*Lake Placid, NY, USA*
*23-28 September, 2007*

[1] On behalf of the LHCb Collaboration.

 

## 1. Introduction

The LHCb experiment is dedicated to study CP violation and other rare phenomena in the decays of beauty particles at the LHC [1]. The LHCb detector covers one side of the forward region. Such a geometry is chosen to ensure efficient flavor tagging, precision decay length measurement, as well as momentum measurement and particle identification. One sub-detector, the Vertex Locator (VELO), plays an important role in tracking and vertex reconstruction. A subset of VELO detector modules equipped with a vacuum and cooling system similar to the final ones, and readout with a prototype of the final DAQ system has been tested in an 180 GeV $\pi$ beam at CERN in 2006. These data are used to optimize various components of this complex system.

In this note I give a brief description of the LHCb detector emphasizing the tracking sub-detectors, an introduction to the LHCb tracking and vertex reconstruction, some results from the VELO testbeam, and the application of vertex reconstruction in LHCb luminosity monitoring.

## 2. The LHCb Detector

The LHCb spectrometer is a one-arm forward detector covering pseudo-rapidity interval $1.9<\eta<4.9$. The schematic layout of the detector is shown in Figure 1. Starting from the interaction region around Z = 0 are the VELO and pile up detector (PU), Ring Imaging Cherenkov detector (RICH1), trigger tracker (TT), tracking stations (T1-3), RICH2, electromagnetic calorimeter (ECAL), hadron calorimeter (HCAL) and muon detectors (M1-5). A dipole magnet sits between the trigger tracker and tracking stations with a bending power of 4 T·m. The magnetic field extends to both trigger tracker and tracking stations.

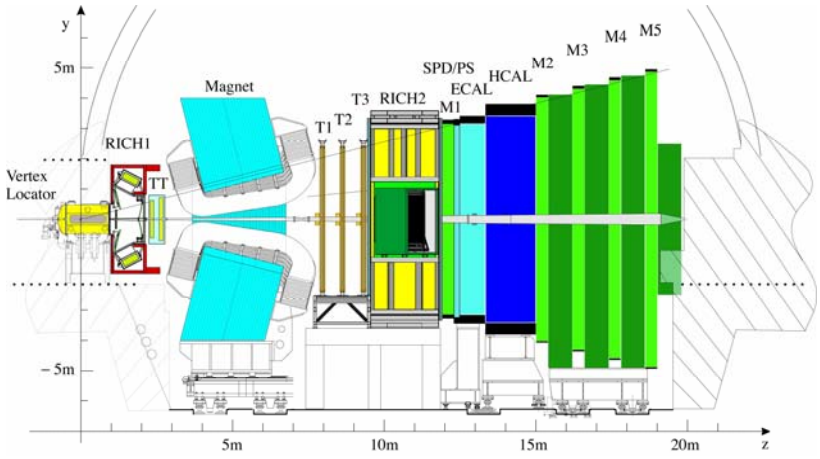


*Figure 1. Skematic layout of the LHCb spectrometer.*

The VELO detector uses silicon strip technology. It is designed to have two halves retractable from the nominal beam line up to 30 mm during beam injection. Each half consists of 21 stations along a ~1 meter length in the beam direction. Each station contains an R-sensor

and a ϕ-sensor in the shape of a half disc. The two sensors are glued to a printed circuit board that is mounted on a carbon fiber support, forming a hybrid. The radial coverage of the sensor is from ~8 mm to ~42 mm. The sensors are $n^+$-on-n type of 300 μm thickness. The R-sensors have concentric strips measuring the radial position of the charged track. The ϕ-sensors have radial inner and outer strips with stereo angles. The ϕ positions are determined from the ϕ strips and projected radial positions. Each sensor has 2048 strips read out through 16 Beetle chips on the hybrid. The strip pitches vary from 40 to 100 μm. This strip design is optimized to reconstruct tracks originating from beam-beam interactions, such that one can reconstruct tracks in the R-Z projection first, and add ϕ hits later.

The trigger tracker is a p-type silicon strip detector, with four planes of different views (0°, +5°, -5°, 0°) and two retractable halves. The sensor has 183 μm strip pitch, and is 500 μm thick. It is inside a small magnetic field with bending power ~ 0.12 T·m. It is important for both long lived particles that can decay after the VELO detector and soft tracks that cannot hit the tracking stations. It also provides $P_t$ information that is essential in the high level trigger [2].

There are 3 tracking stations after the magnet. Each station consists of an inner silicon strip tracker, and an outer straw tube tracker. Both of them have 4 layers of different views, similar to the trigger tracker. The inner tracker covers about 2% of the area close to the beam where the track density is much higher (~20% tracks). Silicon strip detectors similar to the trigger tracker are used with ~200 μm pitch and 320 or 410 μm thickness. The outer tracker handles lower multiplicities using Kapton/Al straw drift tubes of 5 mm diameter.

More details on these three tracking detectors and other sub-detectors are described elsewhere [1].

## 3. Track and Vertex reconstruction at LHCb

The VELO detector is the key element in the LHCb tracking system. Most of the tracks in interesting events produce hits in the VELO. Tracks originating from beam-beam interactions are linear in the R-Z projection, and almost constant in ϕ. Thus the pattern recognition in VELO is done in 2 stages: first in the R-Z projection, and then adding ϕ hits [3].

The procedure of forming R-Z tracks starts from the most downstream plane. A hit in this plane is selected and paired with a hit from the third most downstream plane. The two hits define a straight line, which is required to be consistent with being from the interaction region. A best matched hit from the second most downstream plane is then added to the pair. When a good triplet is found, the line is extrapolated to all the other planes and the best matched hit on each plane is included to form a raw track. Once all combinations of hits from the most downstream plane with hits from the third most downstream plane are exhausted, the algorithm loops over all pairs between the most downstream and the fourth downstream planes to recover any inefficiency. Once this step is complete it starts from the second most downstream plane and so on. Tracks pointing upstream are formed in a similar fashion.

The ϕ hits are added to raw R-Z tracks to form 3-D tracks. The ϕ values are corrected with the projected R values from the raw tracks.

While this procedure is typically quite efficient, it cannot be applied in some special cases where tracks are not originating from the proton-proton interaction region. These include decays of long lifetime particles such as $K_s$, beam monitoring with VELO in open position, or test beam studies. In all these cases tracks are no longer linear in the R-Z plane and $\phi$ is not constant. Special pattern recognition algorithms have been developed for these cases.

Hits in the trigger tracker and the tracking stations are also used in track reconstruction. The tracks reconstructed in the VELO can be used as seeds. The VELO seed tracks are projected to the tracking stations after bending in the magnetic field to form "long tracks". An alternative and supplemental way to form long track is to construct the so called T-tracks in the tracking stations first and then match with VELO seed tracks. About 1/3 of all tracks are long tracks. They have the best quality for physics with good momentum resolution and impact parameter precision. T-tracks that do not match with any VELO seed track may be associated with matched hits in the trigger tracker and form "downstream tracks." These tracks have good momentum resolution and are needed for efficient long lifetime particle reconstruction, e.g. $K_s$. T-tracks that do not match with any VELO seed track or hits in the trigger tracker can provide a momentum measurement, albeit with worse resolution, and are still useful in RICH2 pattern recognition. Some VELO seed tracks may have only matched hits in the trigger tracker. These are soft tracks and contribute to RICH1 pattern recognition. About 1/3 of all tracks have hits only in the VELO. Their momenta are not measured but they are still useful in primary vertex reconstruction.

Tracks are fit with a bi-direction Kalman filter. For long tracks from B decays, the reconstruction efficiency is about 95%, momentum resolution is 0.35% to 0.5%. The impact parameter resolution for high $P_t$ track is about 14 μm. Reconstructed B mass resolution for a typical decay mode is about 15 MeV.

For primary vertex reconstruction, all VELO related tracks are used. A group of these tracks that might come from the same point are selected as seeds. And an iterative fit to a common vertex is implemented, removing the tracks that do not fit in with the rest. Once one primary vertex is formed, a second primary vertex, if there is any, is formed from the rest of the tracks. From MC simulation, the primary vertex reconstruction has an efficiency of about 98% with an 8% fake rate. For typical B decay mode, the primary vertex resolution is about 10 μm in X/Y direction and 50 μm in Z direction; and the B proper time resolution is about 40 fs.

## 4. The 2006 VELO Test Beam

In November of 2006 one partially populated VELO half was tested in a 180 GeV $\pi$ beam. The telescope configuration is shown in Figure 2. In total, 9 final modules and 1 p-on-n type module (leftmost in Figure 2) were mounted inside the vacuum tank. Six of them were read out in each of the several configurations used throughout the data taking. The hybrids were operated inside a vacuum vessel at $10^{-4}$ mbar. A cooling system smaller but similar to the final one was deployed and bi-phase $CO_2$ was used to cool the hybrids. The hybrids were operated at -10°C.

The trigger was provided by 5 scintillation counters positioned up and down-stream of the telescope. The scintillation counters were specially designed for this test beam. The combination logic provided for triggering on two different event topologies: (1) straight-through

beam track events, and (2) events with tracks produced from interactions, such as beam-sensor and beam-target. For straight-through track data, the telescope was angled at 0, 4, and 8 degrees with respect to the beam direction. For interaction events, the telescope was positioned at 0 degrees. The center of the beam was positioned on the sensors, or on pre-mounted lead disc targets. In total 4 small lead discs (d = 2 mm) were placed at the origin of the sensor to mimic beam-gas interactions, and 4 large lead discs (d = 5 mm) at 15 mm away from the origin to mimic the half-open VELO position. The target locations in the beam direction were optimized for detection efficiency. The discs were 200 μm or 300 μm thick.

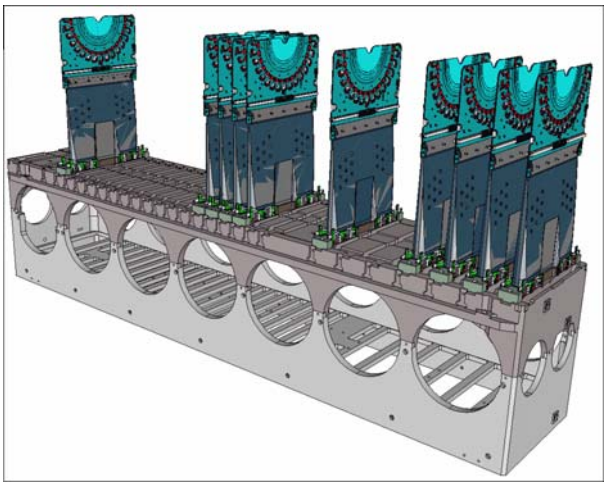

*Figure 2. Telescope configuration of a VELO half as used in the testbeam. 10 hybrids are mounted and 6 of them are readout at a time.*

Nominally, the hybrids were biased at about 100 V, slightly higher than the fully depletion voltage. From each sensor, charge signals collected at 2048 strips were processed by 16 Beetle chips on the hybrid. The differential analog signals were read out through 64 pairs of 60-meter cables, where each handled signals from 32 strips serially. The differential signals were then digitized at a TELL1 electronic board by 10-bit ADCs. In total, 12 TELL1 boards were used; each served one sensor (half station). Digital signals were processed in FPGA chips on TELL1 boards, with running pedestal calculation and zero-suppression. The zero-suppressed data blocks from all TELL1 boards were sent to a Linux PC and time-aligned according to beam crossing (BCO) tags. Events were recorded to hard drives. Raw ADC readouts were also kept in the data stream to test the TELL1 data processing algorithm. Details on the readout data acquisition system (DAQ) are described in a separate paper [4].

The noise performance of one hybrid is shown in Figure 3. The total noise for each channel is shown as the blue line. Signal readouts from 32 strips that share the same data line and ADC were found to have common noise pickup. This coherent common mode fluctuation is removed by averaging the pedestal subtracted ADC values of those channels that have no real signal. The common mode suppressed (CMS) noise is shown as the red line. For a ϕ-sensor the first 683 strips are the inner strips. Each strip has a smaller area compared to the outer ones, but read out through a longer trace. The remaining 1365 strips are outer strips, with shorter traces. About half of them overlap with the readout traces of the inner strips. The three different levels

of noise performance due to these effects are clearly seen. For an R-sensor the structure due to 4 sectors, different strip sizes and trace lengths can also be seen and are well understood. Noise performances of all 10 hybrids are similar. And they are quite stable over runs that span over more than 10 days. The CMS noises are about 1.7–2.2 ADC counts for the ϕ-sensors and 1.9–2.6 ADC counts for the R-sensors, where 1 ADC counts corresponds to roughly 500 electrons. The most probable signal of a minimal ionization particle (MIP) in 300 μm thick silicon is about 50 ADC counts, corresponds to ~24,000 e charge or 86 keV energy deposition. The signal-to-noise ratios are about 24–29 (ϕ-sensors) and 20–24 (R-sensors). This large signal to noise ratio leads to the expectation of good performance even after projected deterioration due to irradiation.

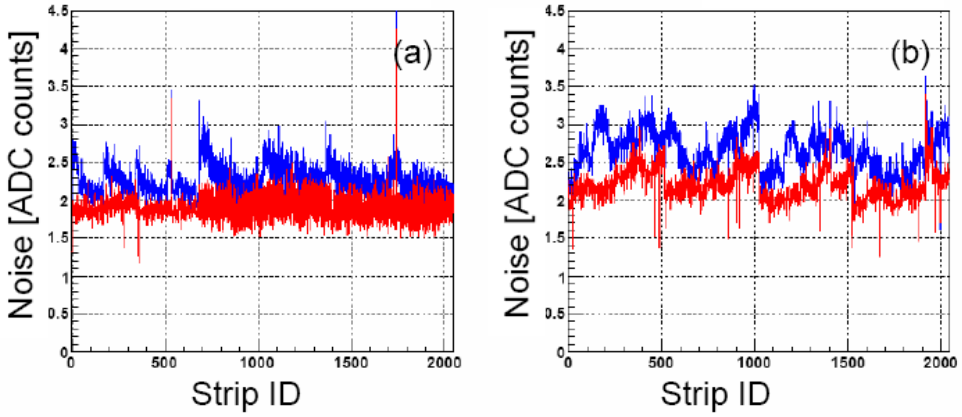


*Figure 3. Distributions of total noise in blue and common mode suppressed noise in red vs strip ID for (a) ϕ-sensor, and (b) R-sensor of a typical hybrid.*

Running pedestal calculation algorithms are used both online and offline. Typically 100 consecutive events are used for the calculation. Within a run of 5000 events that were taken over ~20 s period, the pedestal fluctuation is 0.29 ADC counts. We also compared runs taken over long time intervals. The pedestals are quite stable too, suggesting that we may not need a running calculation.

We observe, however, that pedestals can have very big shifts in a single event. This occurs more often in the interaction triggered data sample than in the straight-through triggered data sample. It is also found that the big shift happens to most channels of a chip coherently, and there are channels in this chip that have very high signals. Figure 4(a) shows this phenomenon in 3 consecutive triggered events: green, red and blue in order. The pedestal shift of chip 5 in the red event is more than 50 ADC counts. About 20 channels apparently have signal. We suspect that the pedestal shift is due to large energy deposition from slow tracks produced in a beam-material interaction. The large signal causes saturation in the amplifier and localized ground or bias shift in the Beetle chip.

Such a shift was reproduced on the test bench, by injecting large test pulses into a few selected channels in a chip. The shift is linear as a function of injected charge. The slope is about -0.12 ADC counts per most probable charge of a MIP.

We estimate this effect in normal LHCb data taking environment using MC simulation. The distribution of chip pedestal shift is shown in Figure 4(b). To quantitatively show the effect

we use two reference criteria: 2 ADC counts, roughly the noise level, and 10 ADC counts, a typical threshold. Out of total 1344 Beetle chips, 7.6 chips per event shift more than 2 ADC counts and 1.2 shift more than 10 ADC counts.

This pedestal shift is like the common mode noise discussed above. The differences are: it affects all channels of the chip; the shift is always negative; the shift can be very large. Considering these features, the signals are recovered with a special algorithm.

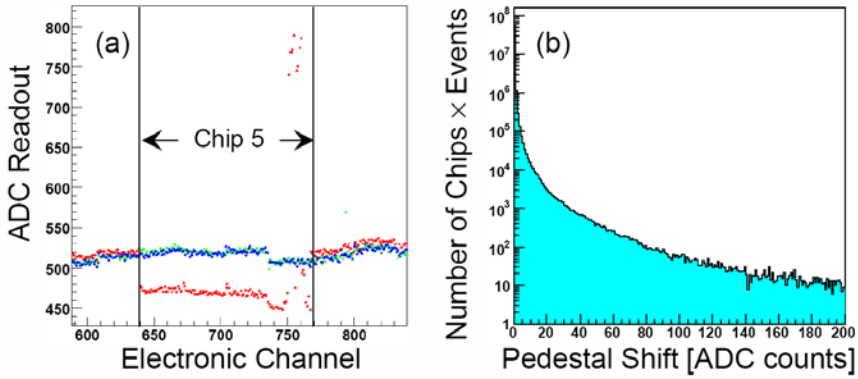


*Figure 4. (a) Testbeam ADC readout value vs electronic channel ID for 3 consecutive events in green, red and blue, and (b) Chip pedestal shift from MC simulation for normal LHCb running.*

Another interesting outcome from these test beam studies is a better understanding of crosstalk between channels. This crosstalk is the modulation of neighbor channel pedestal induced by a signal in a given channel, say, N. It is affected by many factors: the distance from the channel to the hit, asymmetry between channels N-1 and N+1, the phase of the ADC, the sensor type, ϕ-sensor outer strips with or without overlap with inner trace, and so on. Nevertheless, the crosstalk has been studied quite thoroughly, and corrected. The crosstalk can reach ~5% for certain pairs of strips. The correction dramatically improves the residual distribution [5].

There could be more than one strip that has signal due to a single track hit. The spatial position is measured as a centroid with charge weighting. In order to maximally take advantage of charge sharing for spatial resolution, we use a set of three thresholds. We select one or more adjacent strips with individual charge over “seed threshold” and form a cluster seed. The strip adjacent (maximally 2) to the seed is also included in the cluster if it passes “low threshold”. The signal sum of all strips in a cluster must be more than “total charge” threshold. These thresholds are optimized to provide the best efficiency and resolution.

We studied spatial resolution of individual VELO stations through residual distributions. The residual is defined as the difference between the hit position measured at a selected plane and the projection of the track determined by hits of all planes except for the selected one. There are 3 major contributions to the residual spread: the spatial resolution, multiple scattering, and track projection error. The effect of multiple scattering is relatively small and can be estimated from MC simulation. For a track reconstructed in the 0 degree straight track sample, the pitches of strips at different stations are the same; and the spatial resolutions are the same. The track projection error is thus proportional to the spatial resolution, with a calculable scale factor that depends only on relative Z positions of all stations. The preliminary spatial resolutions for

normal incident tracks are shown in Figure 5. Red lines are expected spatial resolutions without charge sharing, i.e. pitch divided by √12. Blue lines are fits to linear function. From the fit the spatial resolution at 40 μm pitch is about 8.4 μm and 8.6 μm, for the ϕ-sensor and R-sensor respectively. The resolution will be further improved after applying non-linear charge sharing between neighboring strips.

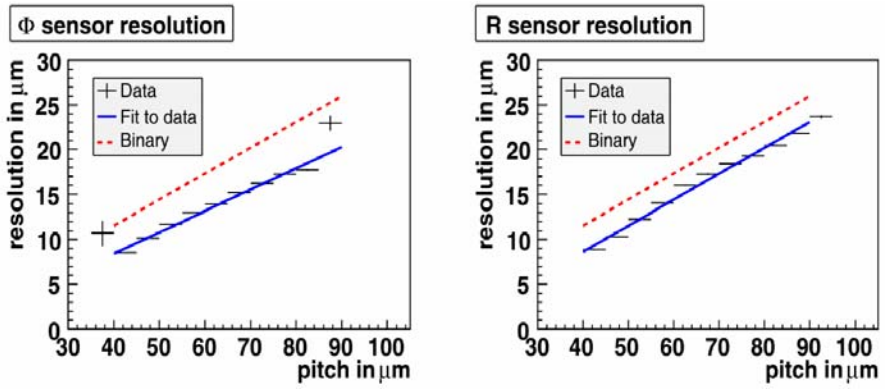


*Figure 5. VELO spatial resolution as function of pitch size for normal incident tracks for (left) ϕ–sensor and (right) R-sensor. Crosses are measurements. Blue solid lines are fits to a linear function. Red dotted lines are expectation without charge sharing.*

The beam particles can interact with material of sensors, targets and the vacuum vessel. We recorded such events with an interaction trigger configuration. Vertices are reconstructed from this data sample to test the reconstruction algorithm. We studied vertex X-Y distributions and obtained the profiles of the target discs, from which we determined edges and estimated lateral resolution. The results are consistent for two different configurations that we read out different set of stations.

## 5. LHCb Luminosity Monitor

Most LHCb physics measurements are relatively independent of absolute luminosity. Some interesting topics, however, rely on it, e.g. W, Z production rate in forward region, inelastic differential cross section, or new physics. Knowledge of the relative luminosity is useful for beam tuning.

LHCb has two methods for relative luminosity monitoring: BRAN-B from the CERN machine group, and the LHCb pileup (PU) detector. BRAN-B uses CdTe disc sensors to measure the flux of neutrons and photons produced in beam-beam interactions. The rate is proportional to luminosity. The PU detector uses silicon strip sensors similar to the VELO R-sensor. It determines the number of primary vertices so that multiple interaction events can be rejected. The rates of the different number of interactions per crossing depend on luminosity. Thus PU can be used to determine relative luminosity through, for example, a zero-counting method. These two detectors can also be used as absolute luminosity monitor providing that the absolute cross-sections are well measured.

The LHCb will study a new method, using VELO in beam-gas events, to determine absolute luminosity [6]. This is an imaging method instead of event counting method. The

lateral profiles of each beam, beam crossing angle and the relative distance between two beams are determined through reconstructed vertices in beam-gas events. With the beam particle populations determined by another method, the absolute luminosity can be calculated. This method requires: (1) the vertex resolutions in X/Y to be substantially smaller than beam transverse sizes; (2) the X/Y dependence of factors that affect the profile measurement to be small or well understood, for example, the gas density and vertex reconstruction efficiency; (3) vertices from the three different sources, viz. beam1-gas, beam2-gas and beam1-beam2 interactions, to be distinguishable.

LHCb will use beam interactions with residual gas in the VELO volume or, if required, with injected gas (e.g. Xenon, since p-Xe interactions give more primary tracks than residual gas nuclei, such as C, O and H). To separate the three different sources, the vertices will be reconstructed in three different regions where each of the three dominates in one region. For a Xe gas pressure of $10^{-7}$ torr and nominal beam particle populations of $10^{11}$ per bunch, the useful event rate is about ~30 Hz for a longitudinal slice of 20 cm. The vertex resolution in X/Y is better than 20 μm, comparing to beam lateral size of ~70 μm. Ultimately the accuracy of this novel method is expected to be limited by the precision of the bunch population measurements.

## 6. Summary and Acknowledgements

LHCb uses the VELO, trigger tracker and tracking stations to measure tracks. Sophisticated algorithms have been developed to reconstruct tracks and vertices. The track momentum resolution is about 0.35-0.5%, and impact parameter resolution is about 14 μm at high $P_t$. LHCb relies on VELO for precision vertex detection. The B proper time resolution is about 40 fs.

A partially populated VELO half was tested in a 180 GeV π beam. The signal-to-noise ratio is about 20 – 29. Spatial resolution is about 8.5 – 25 μm, varying with increasing strip size. Various running experience and knowledge have been obtained through this beam test and VELO algorithms were optimized accordingly.

The fully populated VELO halves have been installed in the interaction hall. The VELO detector is ready for real challenges of LHCb data.

Many colleagues have provided material in preparation of this presentation and proceeding. To them the author owes a debt of gratitude. The author wants to especially thank Drs. M. Artuso, J. Borel, P. Collins, M. Ferro-Luzzi, M. Gersabeck, R. Mountain, M. Needham, A. Papadelis, T. Szumlak, S. Viret and M. Witek for useful discussions.

## References

[1] The LHCb Collaboration, *LHCb Technical Design Report*, CERN- LHCC-2003-030.

[2] T. Bowcock, *Vertex reconstruction and tracking in the trigger algorithm for LHCb*, in proceedings of *Vertex 2007 Workshop* PoS(Vertex2007)032.

[3] D. Hutchcroft, *Velo Pattern Recognition*, CERN-LHCb-2007-13.

[4] N. Neufeld, *Data Acquisition in LHCb VELO Test beams*, in proceedings of *Vertex 2007 Workshop* PoS(Vertex2007)006.

[5] S. Viret, *Alignment strategy for LHCb*, in proceedings of *Vertex 2007 Workshop* PoS(Vertex2007)028.

[6] M. Ferro-Luzzi, *Proposal for an absolute luminosity determination in colliding beam experiments using vertex detection of beam-gas interactions*, Nucl. Instrum. Meth. A**553**, 388 (2005).